

Higgs-boson production in the full theory at NNLO+PS

Marco Niggetiedt and Marius Wiesemann

Max-Planck-Institut für Physik, Boltzmannstraße 8, 85748 Garching, Germany

marco.niggetiedt@mpp.mpg.de, marius.wiesemann@mpp.mpg.de

Abstract

We consider the production of a Standard-Model (SM) Higgs boson in gluon fusion in hadronic collisions and compute the QCD corrections up to next-to-next-to-leading order (NNLO) and match them to parton showers (NNLO+PS). The complete dependence on the top-quark mass is taken into account without making any approximations to the top quark loops mediating the coupling between the gluons and the Higgs boson. To this end, we have included the $gg \rightarrow H$ amplitudes up to three loops and the $pp \rightarrow H + \text{jet}$ amplitudes up to two loops in the full SM theory. This is the first fully differential calculation of the top-quark mass effects up to NNLO in QCD, and we study their impact on relevant observables for the LHC.

1 Introduction

Measurements of the Higgs boson and its properties are one of the cornerstones of the rich physics programme at the Large Hadron Collider (LHC). After its discovery a decade ago [1, 2], the characterization of the Higgs boson has become one of the major quests of the particle physics community. Being naturally the least explored sector in the Standard Model (SM), the Higgs boson offers a large potential for finding discrepancies with the SM in the search for new-physics phenomena. Nevertheless, so far, the measured Higgs couplings to top (t) and bottom (b) quarks, to W and Z bosons, and to τ leptons draw a picture fully consistent with the SM expectation [3, 4]. With the continuously increasing data taking at the LHC, however, the accurate extraction of Higgs properties provides a prime candidate to discover small deviations from SM predictions. To maximize our chances to find such deviation does not only require to reduce the experimental uncertainties through high-statistics measurements, but also to push forward theoretical simulations of LHC collisions to the highest possible precision.

In the SM, Higgs-boson production in hadronic collisions proceeds predominantly through gluon fusion, where the Higgs–gluon coupling is mediated by a heavy-quark loop, with the top quark providing the largest contribution. The most accurate calculations for the gluon-fusion process so far have been done in the approximation of an infinitely heavy top quark, referred to as heavy top limit (HTL). The total inclusive cross section at next-to-next-to-leading order (NNLO) in QCD has been obtained in this approximation already two decades ago [5–7] and even the calculation of the next-to-NNLO ($N^3\text{LO}$) cross section lies quite a few years back [8, 9]. Also several fully-differential calculations in the HTL appeared over the years: at NNLO QCD accuracy for H [10, 11] and $H + \text{jet}$ production [12–15], at NNLO QCD matched to parton showers

(NNLO+PS) [16–19], and recently even at N³LO QCD [20–23]. As far as the quark-mass effects missing in the HTL approximation are concerned, there have been various studies to assess the impact of both the top and the bottom mass in the past at the level of the fully inclusive cross section, see Refs. [24–28], and at the level of the fully differential cross section, see Refs. [29–50]. However, it was only recently that the full dependence on the top-quark mass [51] and on the top-bottom interference [52] was calculated for the total inclusive cross section at NNLO QCD.

In this paper, we present the first differential calculation of NNLO QCD corrections in the full theory, i.e. without any approximations for the top quark mediating the Higgs–gluon interaction, and match them consistently to the parton shower. To this end we employ the MINNLO_{PS} formalism to implement an NNLO+PS generator for the Higgs-boson production in gluon fusion. Being a loop induced process, this calculation entails the full three-loop amplitudes for $pp \rightarrow H$ and the full two-loop amplitudes for $gg \rightarrow H$ +jet production. We study in detail the impact of the complete top-quark mass dependence and assess the quality of previously employed approximations for the top-quark mass effects at NNLO through comparison to our full-theory results.

This letter is organized as follows: We start by outlining the calculation in Section 2 before we discuss the computation of the higher-loop amplitudes in Section 3. Section 4 describes various approximations of the top-mass effects that we use in comparison to our full calculation. Section 5 contains a brief summary of the MINNLO_{PS} method. Phenomenological results are presented in Section 6, and we summarize in Section 7.

2 Outline of the calculation

We consider the process

$$pp \rightarrow H + X, \quad (1)$$

inclusive over the radiation of any extra particles X , and we compute radiative corrections to NNLO QCD in perturbation theory. At LO, Higgs-boson production proceeds via the fusion of two gluons and the Higgs–gluon coupling is induced by a quark loop. The dominant contribution comes from the top quark due to its large Yukawa interaction, see Figure 1 (a) for the corresponding Feynman diagram. At NLO, the virtual contribution is computed from the two-loop $gg \rightarrow H$ amplitude, see Figure 1 (b), and the real contribution corresponds to a one-loop diagram for Higgs production with an extra parton in the final state, i.e. the process $pp \rightarrow Hj$, see Figure 1 (d) for an example. At NNLO, the computation of the three-loop $gg \rightarrow H$ amplitude is required, see Figure 1 (c), the real-virtual contribution corresponding to the two-loop $pp \rightarrow Hj$ amplitude enters, see Figure 1 (e), and the double-real correction has to be included through the one-loop amplitude for Higgs production with two extra partons, i.e. the process $pp \rightarrow Hjj$, see Figure 1 (f) for an example. Using the MINNLO_{PS} method [18, 19], which will be sketched below, we combine the separately divergent amplitudes to compute the NNLO QCD cross section and perform its matching to a parton shower. Note that beyond LO, also diagrams with quarks in the initial state enter the calculation of the cross section, which we do not explicitly depict here.

Our MINNLO_{PS} H generator in the full theory is implemented in the POWHEG-BOX-RES framework [53]. The one-loop-squared amplitudes for the $pp \rightarrow H$, $pp \rightarrow Hj$, and $pp \rightarrow Hjj$ processes are computed through OPENLOOPS [54–56]. To this end, we have extended the OPENLOOPS interface in POWHEG-BOX-RES developed in Ref. [57] to loop-induced processes. The calculation

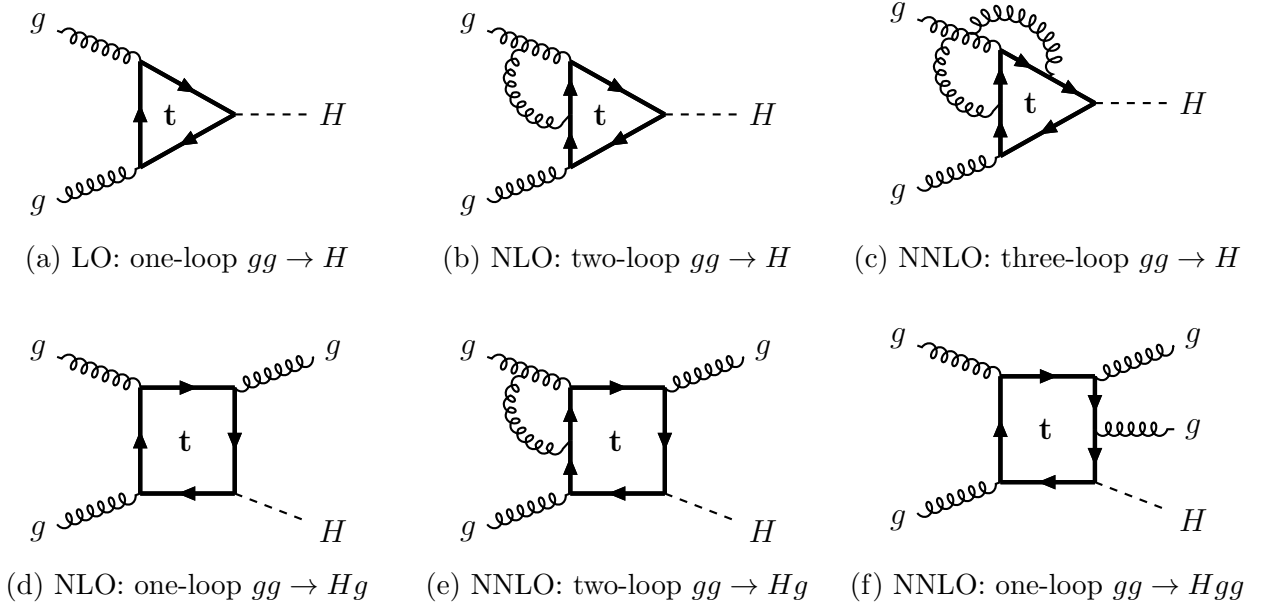


Figure 1: Sample Feynman diagrams entering $pp \rightarrow H$ production up to NNLO.

of the employed two-loop and three-loop amplitudes has been performed in Refs. [51, 58], as described below. The two-loop and three-loop $gg \rightarrow H$ amplitudes are evaluated efficiently through a deep asymptotic expansion in the low-energy limit. The calculation of the two-loop $pp \rightarrow Hj$ contribution is numerically quite intensive and we have derived a dense grid in the phase space and implemented a numerical interpolation based on cubic b-splines. We have checked the validity of the interpolation by performing the same interpolation also for the corresponding one-loop $pp \rightarrow Hj$ amplitude in the HTL by comparing it to the exact result. We provide more details on the calculation of these amplitudes in the following section.

3 Two-loop and three-loop amplitudes

As far as the determination of NNLO corrections including the exact top-quark mass dependence is concerned, the efficient evaluation of the two-loop corrections to the $pp \rightarrow Hj$ process constitutes the main obstacle of the computation due to the rich analytic structure of the underlying Feynman integrals. The workflow of the corresponding calculation has been outlined in Ref. [51]. First, the amplitudes have been reduced to linear combinations of master integrals with the public software `Kira`⊕`FireFly` [59–63]. A particular basis of master integrals suitable for numerical evaluation has been chosen based on the differential equations [64–67], which govern the evolution of the set of master integrals in the space of kinematic invariants and masses. In order to employ the differential equations, an initial condition must be provided, which we obtain from a diagrammatic large-mass expansion [68–71]. It is worth to note that the analytic calculation of the relevant master integrals has previously been addressed in the literature [72–74]. However, even for a subset of planar master integrals the appearance of elliptic sectors has been observed, significantly increasing the complexity of the analytic evaluation. Therefore, we solved the complete set of master integrals numerically in our own framework.

Since the determination of top-quark mass effects is at the core of the study at hand, we

fix the ratio between the mass of the Higgs-boson and the mass of the top-quark according to $m_t^2/m_H^2 = 23/12$, thereby reducing the dimension of the physical parameter space. Without imposing any constraints on the kinematic variables and masses, the parameter space for the two-loop $pp \rightarrow Hj$ amplitudes is spanned by three dimensionless variables (build from the overall four independent dimensionful variables):

$$\rho = \frac{m_t^2}{\hat{s}}, \quad z = 1 - \frac{m_H^2}{\hat{s}}, \quad \lambda = \frac{\hat{t}}{\hat{t} + \hat{u}}, \quad (2)$$

with the standard definition of the Mandelstam variables, \hat{s} , \hat{t} , and \hat{u} . The two-dimensional subspace parametrized in terms of $z \in (0, 1)$ and $\lambda \in (0, 1)$ is probed using the differential equations for the master integrals. More precisely, employing the differential equations in ρ , the initial condition located at $\rho \rightarrow \infty$ is transported to the two-dimensional plane defined by $m_t^2/m_H^2 = \text{const}$. Subsequently, the endpoint of the previous evolution is used as a seed for further evolutions in the directions of z and λ to sample the physical phase space.

It is important to point out that only the phase space region above the top-quark pair threshold needs to be sampled by means of numerical evolutions. For the remaining region including the soft region, we exploit the aforementioned large-mass expansion, which we derived to order $(1/\rho)^{40}$, guaranteeing an efficient evaluation of the amplitudes. We note that the leading term of the expansion corresponds to the HTL and serves as a cross-check for the correctness of our amplitudes.

With the aid of the deep large-mass expansions and the differential equations for numerical evolutions in the z - λ -plane for fixed m_t^2/m_H^2 , we generated dense regular two-dimensional grids in z and λ , which are suitable for the interpolation of the relevant amplitudes $gg \rightarrow Hg$ and $q\bar{q} \rightarrow Hg$ and the permutations of external partons of the latter one. Every grid consists of approximately 7×10^6 high-precision samples of the amplitudes. The grids extend far into the soft and collinear limits, so that no extrapolation is necessary for our purposes. We anticipate that the same grids can also be used in phenomenological applications for slightly different fixed ratios m_t^2/m_H^2 deviating by no more than 1% from the actual ratio without spoiling the outcome of the study. The interpolation is performed through cubic b-splines using the BSPLINE-FORTRAN code¹. The interpolation procedure was validated at the level of the HTL and at the level of the Born amplitude, since for each of them a fast exact implementation exists.

We note that the technology used to obtain the amplitudes for the top quark with a fixed ratio m_t^2/m_H^2 can also be extended to light quark masses. However, due to the smallness of the masses of the bottom and charm quark, only the exact numerical solution of the differential equations is viable, and the corresponding calculation is more involved with regard to the treatment of numerical instabilities. We plan to implement additional grids for the $pp \rightarrow H$ +jet amplitudes at different ratios m_q^2/m_H^2 in future work, specifically for different values of the top-quark, bottom-quark, and charm-quark masses. Furthermore, we reckon that the interpolation of the amplitudes with a fixed mass ratio can subsequently be extended through an additional interpolation in the m_q^2/m_H^2 ratio, hereby relaxing the constraint on the quark mass completely.

Regarding the three-loop double-virtual corrections, the corresponding form factor parametrizing the amplitude for the production of a possibly off-shell Higgs-boson via the scattering of a pair of gluons is available for arbitrary quark flavors circulating in the loops [58, 75]. The form factor is expressed in terms of expansions around special kinematic points and is supplemented by

¹See code under <https://github.com/jacobwilliams/bspline-fortran> developed by Jacob Williams.

high-precision numerical samples. It is sufficient for our application to employ the provided deep asymptotic expansion of the form factor in the low-energy limit as it covers the mass-effects of the top-quark.

4 Approximations of the top-mass effects

Apart from the full-theory implementation retaining the complete dependence on the top-quark loop, we have implemented various approximations for the top quark, which allows us to determine the relevance of the full top-mass effects compared to approximations previously employed in the literature. First of all, we have included the HTL by assuming an infinitely heavy top quark and integrating out the top quark. As a result, in the HTL Feynman diagrams, which due to their simplicity we do not give here explicitly, the top-quark loop in Figure 1 effectively shrinks to a point, inducing a point-like Higgs–gluon vertex in this effective field theory. Therefore, all HTL amplitudes are substantially simpler to calculate as the number of (massive) loops and the number of scales reduces by one. Indeed, the LO diagram in the HTL becomes a tree-level $2 \rightarrow 1$ diagram where the Higgs directly couples to the gluons. For these reasons the HTL has been employed extensively in the past to obtain radiative corrections to Higgs production in gluon fusion, with the most recent advancement being the N³LO corrections in the approximation of an infinitely heavy top quark [8, 9].

Between the most crude approximation of the HTL and the full theory computation there are several intermediate approximations that can be taken. Firstly, the radiative corrections computed in the HTL can be rescaled by the LO $gg \rightarrow H$ cross sections in the full theory (FT), which we shall refer to as HEFT in what follows:

$$d\sigma_{\text{HEFT}}^{\text{NNLO}} = d\sigma_{\text{FT}}^{\text{LO}} \cdot d\sigma_{\text{HTL}}^{\text{NNLO}} / d\sigma_{\text{HTL}}^{\text{LO}}. \quad (3)$$

This approximation, however, only affects the normalization. Differential observables sensitive to a jet in the final state, such as the transverse momentum of the Higgs boson or of the jet, will be described by the HTL amplitude, which is not a good approximation, especially at large transverse momentum. Therefore, we have implemented further approximations of the FT. In all those approximations we keep the one-loop squared Born-level amplitudes for $pp \rightarrow H$, $pp \rightarrow Hj$, and $pp \rightarrow Hjj$ exact, while the two-loop $pp \rightarrow Hj$ amplitudes, which are the most complicated part of our calculation, are computed in the HTL and rescaled differentially by the full $pp \rightarrow Hj$ LO amplitude. We can write this at the level of the finite remainder $|\mathcal{R}_{Hj}\rangle$ of the $pp \rightarrow Hj$ amplitudes as follows:²

$$2 \text{Re}\langle \mathcal{R}_{Hj}^{(0)} | \mathcal{R}_{Hj}^{(1)} \rangle_{\text{FT}} \approx 2 \text{Re}\langle \mathcal{R}_{Hj}^{(0)} | \mathcal{R}_{Hj}^{(1)} \rangle_{\text{HTL}} \cdot \langle \mathcal{R}_{Hj}^{(0)} | \mathcal{R}_{Hj}^{(0)} \rangle_{\text{FT}} / \langle \mathcal{R}_{Hj}^{(0)} | \mathcal{R}_{Hj}^{(0)} \rangle_{\text{HTL}}, \quad (4)$$

where we recall that in the FT $\mathcal{R}_{Hj}^{(0)}$ and $\mathcal{R}_{Hj}^{(1)}$ correspond to diagrams at one-loop and two-loop, respectively, while in the HTL they are obtained from tree-level and one-loop amplitudes, respectively. Additionally, we include three possibilities to approximate the two-loop and three-loop $gg \rightarrow H$ amplitudes. In the first approximation, denoted as FT-approx-1, we apply Eq. (4) and in addition:

$$2 \text{Re}\langle \mathcal{R}_H^{(0)} | \mathcal{R}_H^{(1)} \rangle_{\text{FT}} \approx 2 \text{Re}\langle \mathcal{R}_H^{(0)} | \mathcal{R}_H^{(1)} \rangle_{\text{HTL}} \cdot \langle \mathcal{R}_H^{(0)} | \mathcal{R}_H^{(0)} \rangle_{\text{FT}} / \langle \mathcal{R}_H^{(0)} | \mathcal{R}_H^{(0)} \rangle_{\text{HTL}}, \quad (5)$$

²We define the finite remainder as described in Refs. [76, 77]. Note that this definition should not affect the given approximation.

and

$$\begin{aligned} \langle \mathcal{R}_H^{(1)} | \mathcal{R}_H^{(1)} \rangle_{\text{FT}} &\approx \langle \mathcal{R}_H^{(1)} | \mathcal{R}_H^{(1)} \rangle_{\text{HTL}} \cdot \langle \mathcal{R}_H^{(0)} | \mathcal{R}_H^{(0)} \rangle_{\text{FT}} / \langle \mathcal{R}_H^{(0)} | \mathcal{R}_H^{(0)} \rangle_{\text{HTL}}, \\ 2 \text{Re} \langle \mathcal{R}_H^{(0)} | \mathcal{R}_H^{(2)} \rangle_{\text{FT}} &\approx 2 \text{Re} \langle \mathcal{R}_H^{(0)} | \mathcal{R}_H^{(2)} \rangle_{\text{HTL}} \cdot \langle \mathcal{R}_H^{(0)} | \mathcal{R}_H^{(0)} \rangle_{\text{FT}} / \langle \mathcal{R}_H^{(0)} | \mathcal{R}_H^{(0)} \rangle_{\text{HTL}}, \end{aligned} \quad (6)$$

where $\mathcal{R}_H^{(0)}$, $\mathcal{R}_H^{(1)}$, and $\mathcal{R}_H^{(2)}$ are obtained from one-loop, two-loop, and three-loop amplitudes in the FT, but only constitute to tree-level, one-loop, and two-loop computations in the HTL. The second approximation, denoted as FT-approx-2, is exactly the same as FT-approx-1, but we drop the approximation of the two-loop $gg \rightarrow H$ amplitude in Eq. (5) and take it exact, given that it is known since many years ago [29]. We do exactly the same in our third approximation, denoted as FT-approx-3, but instead of the approximation in Eq. (6) we use the full two-loop $gg \rightarrow H$ amplitude in the rescaling:

$$\begin{aligned} \langle \mathcal{R}_H^{(1)} | \mathcal{R}_H^{(1)} \rangle_{\text{FT}} &\approx \langle \mathcal{R}_H^{(1)} | \mathcal{R}_H^{(1)} \rangle_{\text{HTL}} \cdot 2 \text{Re} \langle \mathcal{R}_H^{(0)} | \mathcal{R}_H^{(1)} \rangle_{\text{FT}} / 2 \text{Re} \langle \mathcal{R}_H^{(0)} | \mathcal{R}_H^{(1)} \rangle_{\text{HTL}}, \\ 2 \text{Re} \langle \mathcal{R}_H^{(0)} | \mathcal{R}_H^{(2)} \rangle_{\text{FT}} &\approx 2 \text{Re} \langle \mathcal{R}_H^{(0)} | \mathcal{R}_H^{(2)} \rangle_{\text{HTL}} \cdot 2 \text{Re} \langle \mathcal{R}_H^{(0)} | \mathcal{R}_H^{(1)} \rangle_{\text{FT}} / 2 \text{Re} \langle \mathcal{R}_H^{(0)} | \mathcal{R}_H^{(1)} \rangle_{\text{HTL}}. \end{aligned} \quad (7)$$

Of course, there is a certain level of ambiguity involved, depending on how the finite remainders are defined in detail. However, FT-approx-1, FT-approx-2, FT-approx-3 are approximations that were feasible also without the complete computation in the FT, and they allow us to determine the robustness of such approximations by comparing them to the full result. This can be useful not only to validate legacy Higgs calculations that were applied previously, but also in view of applying such approximations beyond NNLO, and in particular to the production of a Higgs boson with higher multiplicities, such as $pp \rightarrow Hjj$ production in gluon fusion.

5 MiNNLO_{PS} method

In the following, we provide a brief summary of the MiNNLO_{PS} method for colour-singlet production, which was originally developed in Refs. [18, 19] and has been applied to several processes by now [78–86]. MiNNLO_{PS} is also the only NNLO+PS method that has been extended to processes with colour charges in initial and final state, namely heavy-quark pair production [87–89], and very recently to the associated production of a heavy-quark pair and a colour singlet in Ref. [90], where it was applied to $b\bar{b}Z$ production.

Starting from a POWHEG [91–94] NLO+PS calculation for the production of a colour singlet (F) with a jet, the MiNNLO_{PS} master formula can be expressed as

$$d\sigma_{\text{F}}^{\text{MiNNLO}_{\text{PS}}} = d\Phi_{\text{FJ}} \bar{B}^{\text{MiNNLO}_{\text{PS}}} \times \left\{ \Delta_{\text{pwg}}(\Lambda_{\text{pwg}}) + d\Phi_{\text{rad}} \Delta_{\text{pwg}}(p_{\text{T,rad}}) \frac{R_{\text{FJ}}}{B_{\text{FJ}}} \right\}, \quad (8)$$

where the \bar{B} function of POWHEG is modified in such a way that it yields NNLO QCD accuracy for the production of F in the limit where QCD radiation becomes unresolved

$$\bar{B}^{\text{MiNNLO}_{\text{PS}}} = e^{-S} \left\{ \frac{d\sigma_{\text{FJ}}^{(1)}}{d\Phi_{\text{FJ}}} (1 + S^{(1)}) + \frac{d\sigma_{\text{FJ}}^{(2)}}{d\Phi_{\text{FJ}}} + (D - D^{(1)} - D^{(2)}) \times F^{\text{corr}} \right\}. \quad (9)$$

Here, Φ_{FJ} denotes the FJ phase space, Δ_{pwg} is the POWHEG Sudakov, and Φ_{rad} and $p_{\text{T,rad}}$ are the phase space and the transverse momentum of the second radiation. B_{FJ} and R_{FJ} are determined by

the squared tree-level matrix elements for FJ and FJJ production, respectively. In Eq. (9), $d\sigma_{\text{FJ}}^{(1,2)}$ denote the first- and second-order differential FJ cross section. All other contributions originate from the transverse-momentum (p_{T}) resummation formula, as explained in section 4 of Ref. [18],

$$d\sigma_{\text{F}}^{\text{res}} = \frac{d}{dp_{\text{T}}} \{e^{-S} \mathcal{L}\} = e^{-S} \underbrace{\{-S' \mathcal{L} + \mathcal{L}'\}}_{\equiv D}, \quad (10)$$

which defines the function D in Eq. (9), and e^{-S} is the Sudakov form factor, $S^{(1)}$ is the $\mathcal{O}(\alpha_{\text{S}})$ term in the expansion of its exponent, \mathcal{L} denotes the luminosity factor up to NNLO, which includes the convolution of the collinear coefficient functions with the parton distribution functions (PDFs) and the squared hard-virtual matrix elements for F production. Note that within the MINNLO_{PS} approach renormalization and factorization scales are set to p_{T} , except for the two overall powers of α_s , whose scale can be chosen arbitrarily.

The last term of the \bar{B} function in Eq. (9), which is of order $\alpha_{\text{S}}^3(p_{\text{T}})$, adds the relevant (singular) contributions necessary to reach NNLO accuracy [18], while regular contributions in p_{T} are subleading at this order. Note that, instead of truncating the singular contributions included through D at α_{S}^3 , i.e. $(D - D^{(1)} - D^{(2)}) = D^{(3)} + \mathcal{O}(\alpha_{\text{S}}^4)$, as in the original MINNLO_{PS} formulation of Ref. [18], we follow the extension introduced in Ref. [19] and preserve the total derivative in Eq. (10). This allows us to keep subleading logarithmic contributions beyond $\mathcal{O}(\alpha_{\text{S}}^3)$ that are relevant to achieve a better agreement with fixed-order NNLO results. The factor F^{corr} in Eq. (9) implements an appropriate functional form to spread $(D - D^{(1)} - D^{(2)})$, which has Born-like kinematics, in Φ_{FJ} within our event generator [18].

Finally, the MINLO' cross section is defined by simply dropping the last term of Eq. (9), which includes the NNLO corrections. Thereby, one achieves a merging of 0-jet and 1-jet multiplicities at NLO QCD accuracy.

6 Results

We present phenomenological results of our new MINNLO_{PS} generator for Higgs production in gluon fusion in the full theory at the LHC with 13 TeV centre-of-mass energy. To study the effect of the full top-mass dependence in our calculation, we consider both the case of an on-shell Higgs boson and the one where the $H \rightarrow \gamma\gamma$ decay is included in the zero-width approximation through the parton shower, with realistic fiducial cuts on the photons as applied by the experiments.

For the input parameters we set a Higgs mass of $m_H = 125$ GeV. The top-quark is treated in the on-shell scheme with a mass of $m_t = 173.2$ GeV and a width of $\Gamma_t = 1.44262$ GeV. We use $n_f = 5$ massless quark flavours and the corresponding NNLO PDF set with $\alpha_{\text{S}}(m_Z) = 0.118$ of NNPDF3.1 [95]. The renormalization scale of the two overall powers of the strong coupling is set to the Higgs mass $\mu_R^{(0)} = K_R m_H$. For the extra powers of the strong coupling and the factorization scale, we follow the standard MINNLO_{PS} scale settings described in Ref. [19], which effectively sets $\mu_R \sim K_R p_{\text{T}}$ and $\mu_F \sim K_F p_{\text{T}}$ at small transverse momentum. The central scale setting corresponds to $K_R = K_F = 1$, while scale uncertainties are estimated by varying K_R and K_F up and down by a factor of two with the constraint $1/2 \leq K_R/K_F \leq 2$. For the technical settings of the MINNLO_{PS} predictions we employ modified logarithms that smoothly turn off the resummation effects at large transverse momenta using the setting `modlog_p 6` in the POWHEG

	σ_{total} [pb]	ratio to NNLO QCD
NNLO QCD	40.32(2) $^{+10.4\%}_{-10.7\%}$	1.000
MINLO'	31.16(1) $^{+22.9\%}_{-17.6\%}$	0.773
MINNLO _{PS}	39.55(1) $^{+11.0\%}_{-10.5\%}$	0.981

Table 1: Total cross section in the HTL at NNLO QCD compared to MINLO' and MINNLO_{PS}.

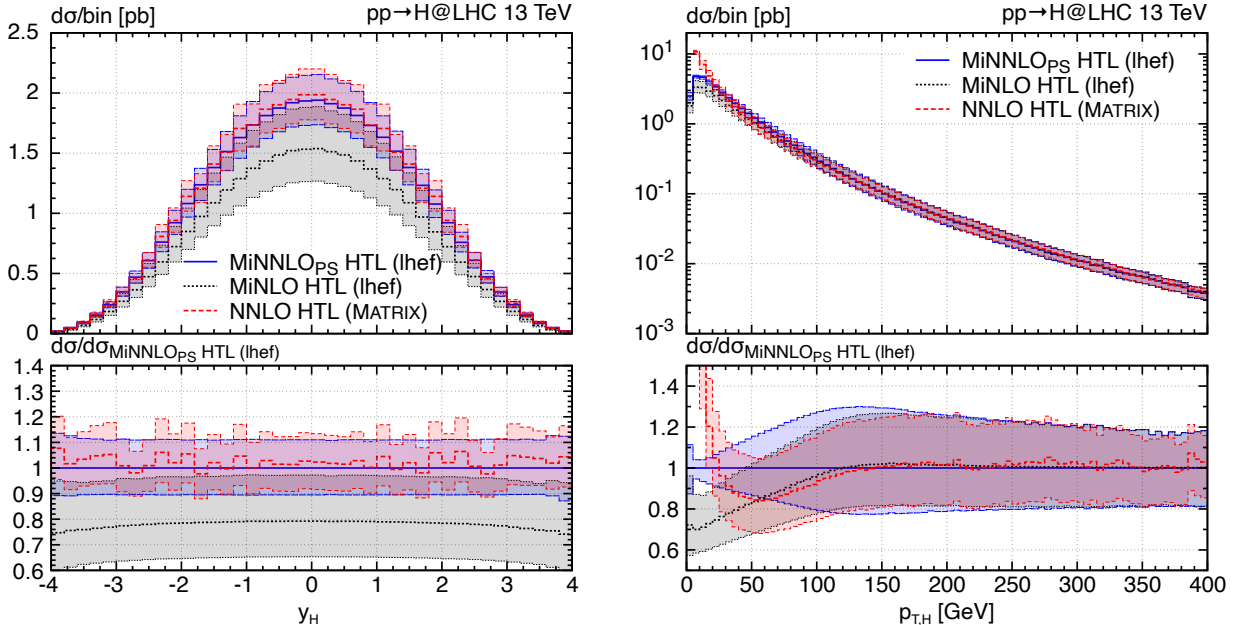


Figure 2: Comparison of MINNLO_{PS} and MINLO' predictions with fixed-order NNLO results.

input card, with an associated scale of $Q = K_Q m_h$ with $K_Q = 1$. And we smoothly avoid the Landau singularity by multiplying the unphysical scales by a profile function at small transverse, using $Q_0 = 2$ [19].

All MINNLO_{PS} results are showered with PYTHIA8 [96], switching off hadronization and underlying event. Besides on-shell Higgs results we also study Higgs-boson decays to two photons, which we model through PYTHIA8 assuming a branching fraction of $\text{BR}(H \rightarrow \gamma\gamma) = 0.00227$. While no cuts are used in the on-shell case, for the diphoton final states we compare the fully inclusive case and two fiducial setups with typical selection criteria [97]. In both fiducial setups we require a rapidity threshold of $|\eta_\gamma| < 1.37$ or $1.52 < |\eta_\gamma| < 2.37$. For the the transverse momentum of the photons we consider both asymmetric cuts with $p_{T,\gamma_1} > 0.35 m_H$ and $p_{T,\gamma_2} > 0.25 m_H$, dubbed **fid-asym-cuts**, and product cuts such that $\sqrt{p_{T,\gamma_1} p_{T,\gamma_2}} > 0.35 m_H$ and $p_{T,\gamma_2} > 0.25 m_H$, as suggested in Ref. [98], dubbed **fid-prod-cuts**.

We obtain reference NNLO results from MATRIX [99] in the HTL with the same input setup. For the unphysical scales we set $\mu_R^{(0)} = \mu_R \sim K_R m_H$ and $\mu_F \sim K_F m_H$, and the central scale and the scale variations are obtained as described above.

We start by validating our new implementation of the MINNLO_{PS} H generator in POWHEG-BOX-RES against fixed-order NNLO QCD predictions in the HTL. Shower effects are turned off in

	σ_{total} [pb]	ratio to HTL
HTL	39.55(1) $^{+11.0\%}_{-10.5\%}$	1.000
HEFT	42.13(1) $^{+11.0\%}_{-10.5\%}$	1.065
FT	42.01(1) $^{+11.2\%}_{-10.6\%}$	1.062
FT-approx-2	41.73(1) $^{+10.9\%}_{-10.4\%}$	1.055
FT-approx-3	41.76(1) $^{+10.9\%}_{-10.4\%}$	1.056

Table 2: Total cross sections predicted by $\text{MiNNLO}_{\text{PS}}$ in various approximations.

this comparison by using results at Les-Houches-Event (LHE) level for a more direct comparison to fixed order. The total cross sections at fixed-order NNLO QCD and predicted by $\text{MiNNLO}_{\text{PS}}$, given in Table 1, lie within 2%, and therefore agree well within the given uncertainties. We recall that the two predictions differ in the treatment of terms beyond accuracy and are not expected to yield the same numerical result. The MINLO' cross section, on the other hand, is more than 20% lower, and features substantially larger scale uncertainties.

In Figure 2, we show the same comparison for differential distributions. The NNLO QCD prediction of MATRIX is represented by a red, dashed curve with a red band, while the MINLO' and $\text{MiNNLO}_{\text{PS}}$ predictions are shown in black, dotted and blue, solid, respectively. For the rapidity distribution of the Higgs boson (y_H) in the left figure, we observe excellent agreement within the quoted scale uncertainties between the $\text{MiNNLO}_{\text{PS}}$ and NNLO QCD histograms. The scale uncertainties are of the same size (about $\sim 10\%$) and the central values agree at the level of 1-2%. Compared to the MINLO' prediction we observe relatively flat $\text{MiNNLO}_{\text{PS}}$ corrections of about +25% and a smaller scale-uncertainty band. For the Higgs transverse-momentum ($p_{T,H}$) spectrum in the right figure, on the other hand, $\text{MiNNLO}_{\text{PS}}$ and NNLO QCD results agree at large $p_{T,H}$. At small $p_{T,H}$ the fixed-order prediction diverges due to the large logarithmic contributions, while MINLO' and $\text{MiNNLO}_{\text{PS}}$ predictions remain finite. Note that at large $p_{T,H}$ all three predictions are formally only NLO accurate and coincide with each other. It is interesting to observe the typical pattern that the corrections included through $\text{MiNNLO}_{\text{PS}}$ with respect to MINLO' all enter the cross section at small $p_{T,H}$ and are then smoothly turned off. This is physically appropriate and a direct consequence of the NNLO+PS matching approach and the employed modified logarithms.

After having validated our $\text{MiNNLO}_{\text{PS}}$ event generator for Higgs-boson production, we now analyze the effect of including the exact top-mass dependence at NNLO in QCD. Table 2 shows the total inclusive cross section predicted by our $\text{MiNNLO}_{\text{PS}}$ generator in various approximations, HTL, HEFT, FT, FT-approx-2, and FT-approx-3. The HEFT result corresponds to the HTL result rescaled by exact top-mass dependence at LO, as given in Eq. (3). Comparing the full theory (FT) result against the HTL one, we find mass effects of about 6.2%. Accounting for the mass effects at LO, and thus comparing the FT prediction against the HEFT approximation, we see that the FT is lower than the HEFT one by only -0.3%. This confirms the effect that has been found in the study of the total inclusive NNLO QCD cross section at fixed order in Ref. [51]. Moreover, we can also conclude from Table 2, that the approximations introduced in Section 4, namely FT-approx-2 and FT-approx-3, provide a good approximation of the top-mass effects for the total inclusive cross section, being only 0.6–0.7% lower than the FT cross section.³

³Notice that FT-approx-1 is so close to the other two results that we refrain from including it here and in the following.

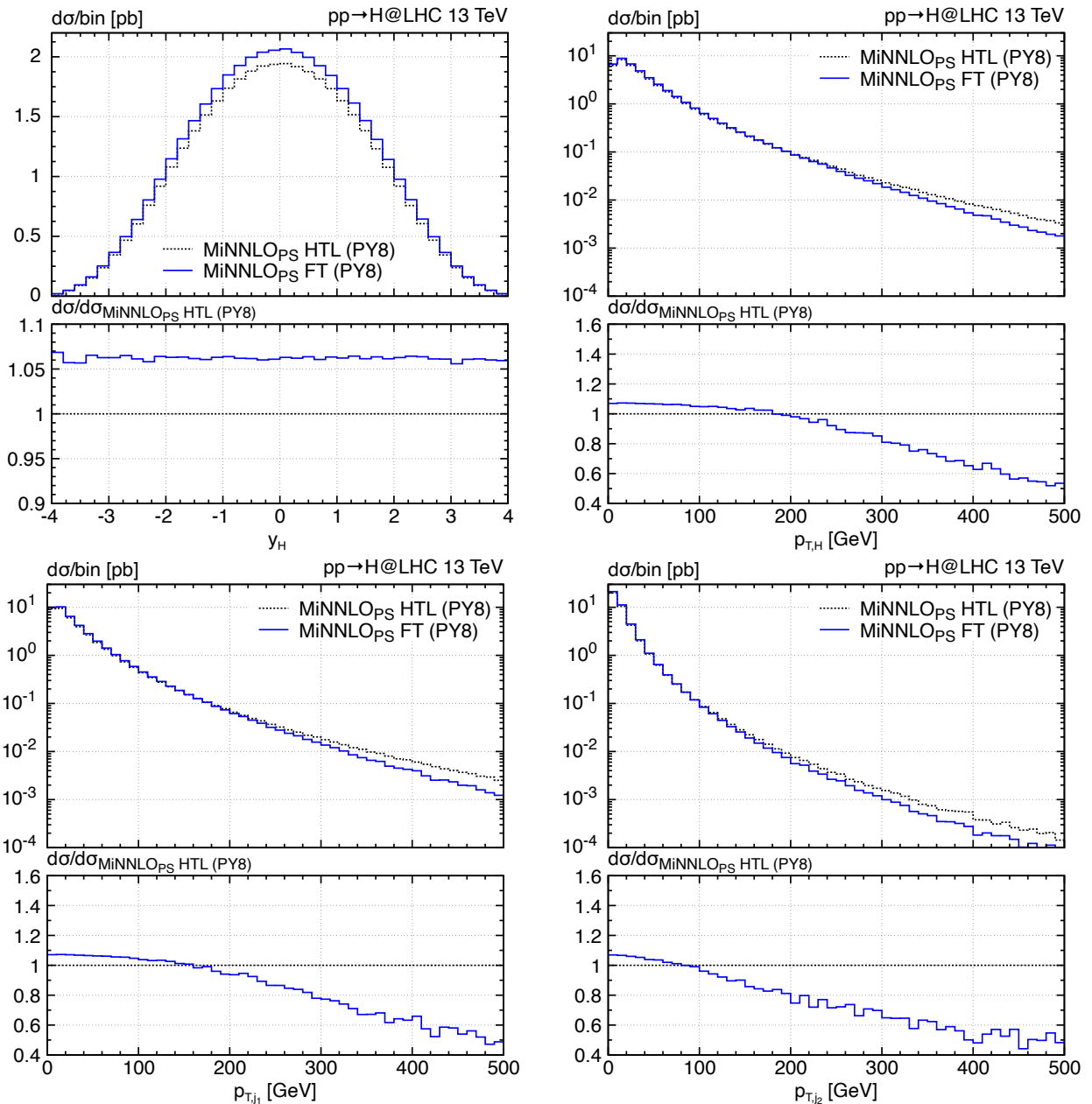


Figure 3: Top-mass effects in the FT compared to the HTL for MiNNLO_{PS} predictions.

We continue by analyzing the mass effects in differential distributions in Figure 3. Note that the full theory (FT) results, shown as a blue, solid curve, have been obtained from the HTL results, shown in black, dotted curve, by reweighting the Les-Houches events to the complete calculation, since the FT matrix elements are substantially slower. This approach is exact in the limit of large statistics, bearing that it does not entail any approximation beyond the (very small) numerical uncertainties. The top-quark mass effects can be read off the blue FT/HTL ratio curve in the lower panels of the figures. In the y_H distribution the effect is completely flat and about +6%, as already observed for the total inclusive cross section in Table 2. In the transverse momentum distribution of the Higgs boson (upper right figure), of the leading jet (p_{T,j_1} , lower left figure) and of the subleading jet (p_{T,j_2} , lower right figure), the top-mass effects show a very similar behaviour.

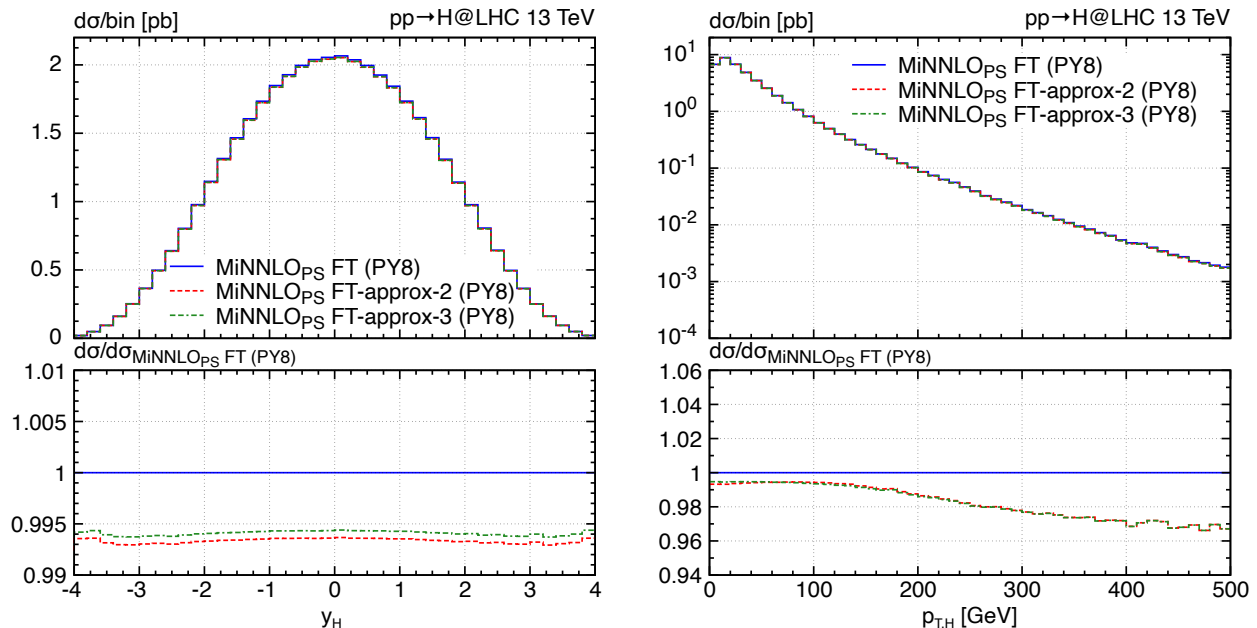


Figure 4: Comparison of top-mass approximations to the FT result for $\text{MiNNLO}_{\text{PS}}$ predictions.

At small p_T the effect is about +6%, while the top-mass dependence steadily decreases the cross section in the transverse-momentum tails, halving the $\text{MiNNLO}_{\text{PS}}$ cross section in the HTL approximation around 500 GeV. This feature is well known and related to the fact that at large transverse momentum the top quarks in the loop get resolved, leading to a smaller cross section.

Next, we would like to assess the quality of the different approximations of the top-mass dependence in the $\text{MiNNLO}_{\text{PS}}$ cross section, defined in Section 4, which could be applied already before our calculation in the full theory of this manuscript. To this end, we compare the complete top-mass dependence in $\text{MiNNLO}_{\text{PS}}$ (blue, solid) with the corresponding implementations of the approximations FT-approx-2 (red, dashed curve) and FT-approx-3 (green, double-dash-dotted curve) in Figure 4. We find that for inclusive NNLO observables, i.e. the inclusive cross section and the Higgs rapidity distribution (left figure), the approximations of the FT work perfectly and differ from the full result by only about six permille. This also holds true for small $p_{T,H}$ values. On the other hand, we can observe that at large $p_{T,H}$ the approximations successively differ more from the exact result, reaching about 3% at $p_{T,H} = 500$ GeV. Nevertheless, the approximations work at a very satisfactory level, especially considering the scale uncertainties, which are much larger. The corresponding figures for other transverse-momentum observables, like p_{T,j_1} and p_{T,j_2} , show the same (relative) behaviour as for $p_{T,H}$, which is why we refrain from showing them here, and, thus, the same conclusions apply to them.

We now move on from discussing results for stable Higgs bosons to including the Higgs decay to photons. In Figure 5 we consider including the full top-mass dependence compared to the HTL by showing representative results for the $p_{T,H}$ spectrum, where the Higgs boson is reconstructed from the two photons, and for the transverse-momentum distribution of the leading photon (p_{T,γ_1}). Very similar top-mass effects can be observed for other transverse-momentum observables of the jets and the subleading photon. Three different scenarios are considered for applying fiducial cuts on the photons, as introduced above: no cuts (left column), with asymmetric cuts on the photons (*fid-asym-cuts*, center column), with product cuts on the photons (*fid-prod-cuts*,

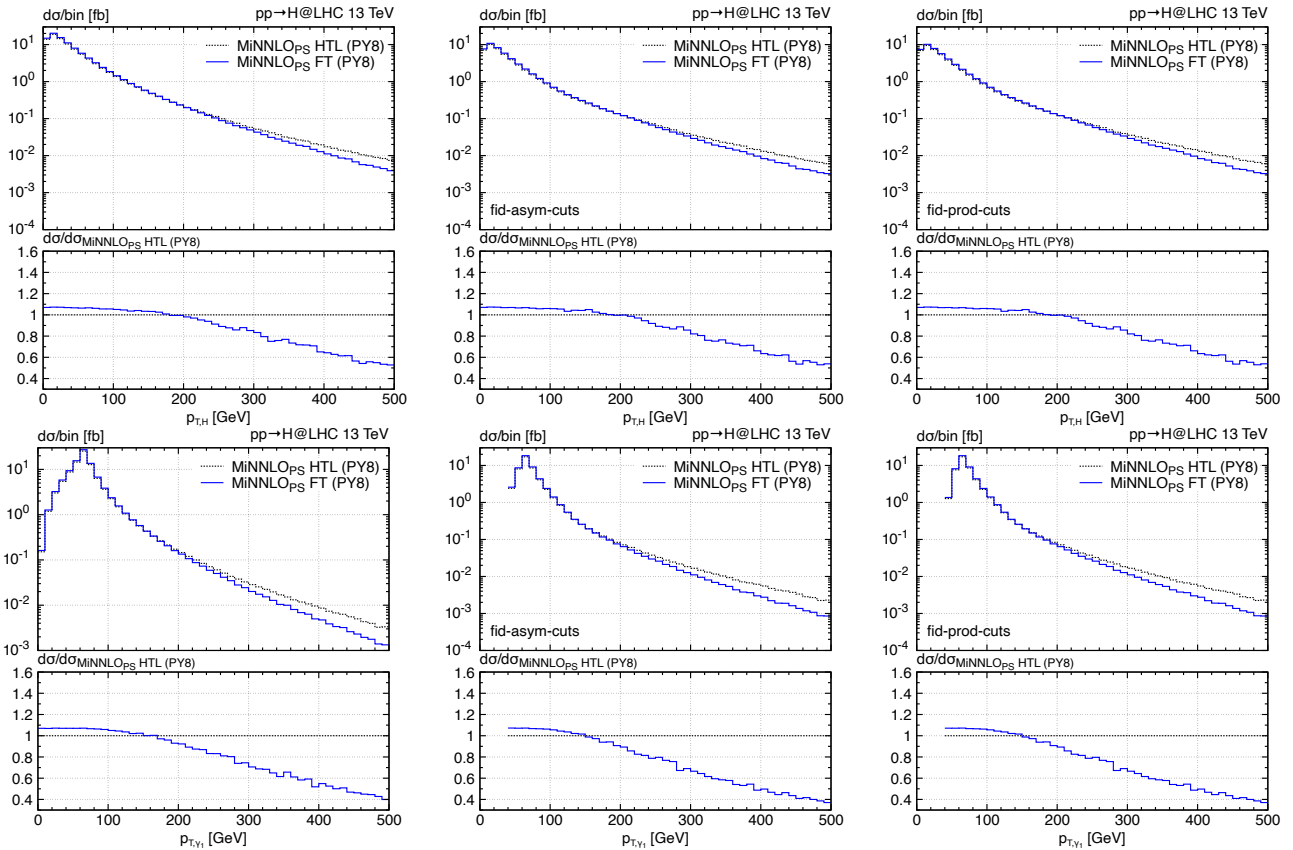


Figure 5: Top-mass effects in distributions of diphoton predictions obtained via $\text{MiNNLO}_{\text{PS}}$.

right column). We observe that the size of top-mass effects does not depend on the cuts applied to the photons in these scenarios. Moreover, we find a slightly larger dependence on the top mass in the tail of the p_{T,γ_1} distribution compared to the $p_{T,H}$ spectrum, but the qualitative behaviour is very similar.

Finally, we show in Figure 6 that also the quality of the different approximations of the top-mass effects does not depend on the fiducial selection cuts applied to the photons. Moreover, the approximations of the FT result work slightly worse for the p_{T,γ_1} spectrum compared to the $p_{T,H}$ one. The difference to the FT prediction reaches about 4% for $p_{T,\gamma_1} = 500$ GeV, while it is about 3% for $p_{T,H} = 500$ GeV.

7 Summary

We have presented the calculation of Higgs-boson production through gluon fusion in the full theory at NNLO in QCD and matched it to a parton shower with the $\text{MiNNLO}_{\text{PS}}$ method. For the first time, NNLO QCD corrections are computed at the fully differential level without any approximations for the top-quark loop, i.e. taking into account the complete dependence on the top-quark mass. Hence, our calculation includes $gg \rightarrow H$ amplitudes up to three loops and $pp \rightarrow H$ +jet amplitudes up to two loops in the full SM theory.

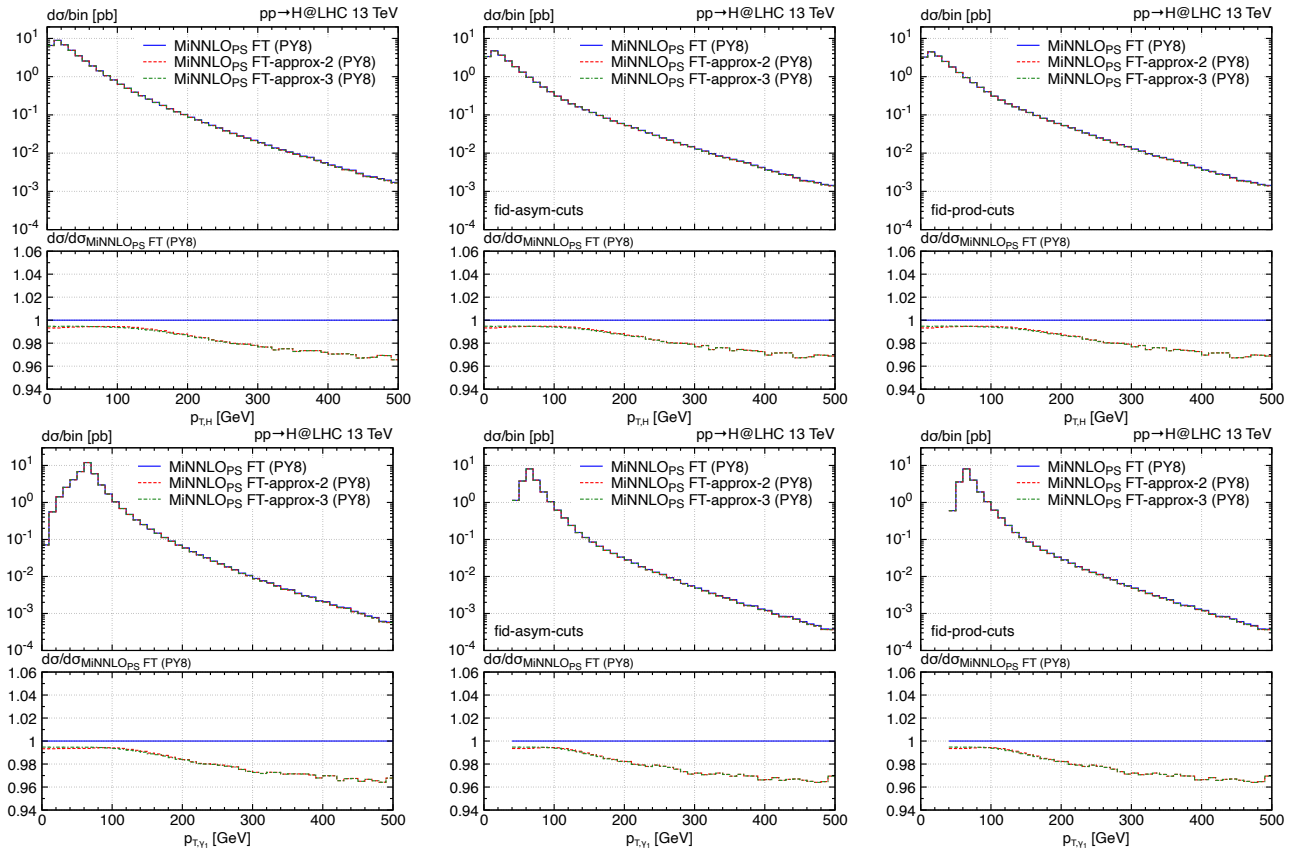


Figure 6: Quality of top-mass approximations in diphoton distributions of $\text{MiNNLO}_{\text{PS}}$ predictions.

We have studied the effect of the top-quark mass on our $\text{MiNNLO}_{\text{PS}}$ predictions with respect to the approximation of an infinitely heavy top quark both for a stable Higgs boson and including its decay to photons. We find the impact of the top-quark mass to be about +6% on the total inclusive cross section and completely flat in the Higgs rapidity spectrum at NNLO QCD. Since the relative impact is the exact same as the one already at the leading order, a rescaling of the HTL with Born $gg \rightarrow H$ amplitude provides an excellent approximation of the full theory result for NNLO observables. Considering transverse-momentum spectra of the Higgs boson, the jets or the decay photons, on the other hand, the top-quark mass yields a large negative effect that continuously increases in the tail of these distributions, reducing the cross section by a factor of two and more at transverse-momentum scales of around 500 GeV. We have also shown that these large effects in the full SM theory can be largely captured through various approximations that employ a rescaling of the HTL amplitudes with lower-order amplitudes including the complete top-mass dependence. The differences between these approximations and the full result are less than 5% around transverse momenta of 500 GeV and only at the few-permille level for inclusive NNLO observables, which is very small compared to the uncertainties due to missing higher-order corrections.

Our analysis reflects that it is indispensable to include top-mass effects in state-of-the-art simulations of Higgs-boson production through gluon fusion, but it also shows the high quality of previously employed approximations of these effects. Our newly developed $pp \rightarrow H$ $\text{MiNNLO}_{\text{PS}}$ generator at NNLO+PS in the full theory constitutes the most accurate tool to model signal

events of the Higgs boson at the LHC, and we reckon that it will be a useful addition to ongoing and future experimental analyses. With the development of this generator we pave the way for including also subleading quark-mass effects, such as those originating from bottom-quark and charm-quark loops, whose inclusion we leave to future work. Although more challenging, the calculation for light quarks can be approached in a very similar manner.

Acknowledgements. We would like to thank Michał Czakon, Robert Harlander and Giulia Zanderighi for fruitful discussions. We are also indebted to Robert Harlander and Giulia Zanderighi for comments on the manuscript.

References

- [1] ATLAS collaboration, *Observation of a new particle in the search for the Standard Model Higgs boson with the ATLAS detector at the LHC*, *Phys. Lett. B* **716** (2012) 1 [[1207.7214](#)].
- [2] CMS collaboration, *Observation of a New Boson at a Mass of 125 GeV with the CMS Experiment at the LHC*, *Phys. Lett. B* **716** (2012) 30 [[1207.7235](#)].
- [3] ATLAS collaboration, *A detailed map of Higgs boson interactions by the ATLAS experiment ten years after the discovery*, *Nature* **607** (2022) 52 [[2207.00092](#)].
- [4] CMS collaboration, *A portrait of the Higgs boson by the CMS experiment ten years after the discovery.*, *Nature* **607** (2022) 60 [[2207.00043](#)].
- [5] R.V. Harlander and W.B. Kilgore, *Next-to-next-to-leading order Higgs production at hadron colliders*, *Phys.Rev.Lett.* **88** (2002) 201801 [[hep-ph/0201206](#)].
- [6] C. Anastasiou and K. Melnikov, *Higgs boson production at hadron colliders in NNLO QCD*, *Nucl.Phys.* **B646** (2002) 220 [[hep-ph/0207004](#)].
- [7] V. Ravindran, J. Smith and W.L. van Neerven, *NNLO corrections to the total cross-section for Higgs boson production in hadron hadron collisions*, *Nucl.Phys.* **B665** (2003) 325 [[hep-ph/0302135](#)].
- [8] C. Anastasiou, C. Duhr, F. Dulat, F. Herzog and B. Mistlberger, *Higgs Boson Gluon-Fusion Production in QCD at Three Loops*, *Phys. Rev. Lett.* **114** (2015) 212001 [[1503.06056](#)].
- [9] B. Mistlberger, *Higgs boson production at hadron colliders at N³LO in QCD*, *JHEP* **05** (2018) 028 [[1802.00833](#)].
- [10] C. Anastasiou, K. Melnikov and F. Petriello, *Higgs boson production at hadron colliders: Differential cross sections through next-to-next-to-leading order*, *Phys. Rev. Lett.* **93** (2004) 262002 [[hep-ph/0409088](#)].
- [11] S. Catani and M. Grazzini, *An NNLO subtraction formalism in hadron collisions and its application to Higgs boson production at the LHC*, *Phys. Rev. Lett.* **98** (2007) 222002 [[hep-ph/0703012](#)].
- [12] R. Boughezal, F. Caola, K. Melnikov, F. Petriello and M. Schulze, *Higgs boson production in association with a jet at next-to-next-to-leading order in perturbative QCD*, *JHEP* **06** (2013) 072 [[1302.6216](#)].
- [13] X. Chen, T. Gehrmann, E.W.N. Glover and M. Jaquier, *Precise QCD predictions for the production of Higgs + jet final states*, *Phys. Lett.* **B740** (2015) 147 [[1408.5325](#)].
- [14] R. Boughezal, F. Caola, K. Melnikov, F. Petriello and M. Schulze, *Higgs boson production in*

- association with a jet at next-to-next-to-leading order, *Phys. Rev. Lett.* **115** (2015) 082003 [1504.07922].
- [15] X. Chen, J. Cruz-Martinez, T. Gehrmann, E.W.N. Glover and M. Jaquier, *NNLO QCD corrections to Higgs boson production at large transverse momentum*, *JHEP* **10** (2016) 066 [1607.08817].
- [16] K. Hamilton, P. Nason, E. Re and G. Zanderighi, *NNLOPS simulation of Higgs boson production*, *JHEP* **10** (2013) 222 [1309.0017].
- [17] S. Höche, Y. Li and S. Prestel, *Higgs-boson production through gluon fusion at NNLO QCD with parton showers*, *Phys. Rev.* **D90** (2014) 054011 [1407.3773].
- [18] P.F. Monni, P. Nason, E. Re, M. Wiesemann and G. Zanderighi, *MiNNLO_{PS}: A new method to match NNLO QCD to parton showers*, *JHEP* **05** (2020) 143 [1908.06987].
- [19] P.F. Monni, E. Re and M. Wiesemann, *MiNNLO_{PS}: optimizing $2 \rightarrow 1$ hadronic processes*, *Eur. Phys. J. C* **80** (2020) 1075 [2006.04133].
- [20] L. Cieri, X. Chen, T. Gehrmann, E.W.N. Glover and A. Huss, *Higgs boson production at the LHC using the q_T subtraction formalism at N^3LO QCD*, *JHEP* **02** (2019) 096 [1807.11501].
- [21] F. Dulat, B. Mistlberger and A. Pelloni, *Precision predictions at N^3LO for the Higgs boson rapidity distribution at the LHC*, *Phys. Rev.* **D99** (2019) 034004 [1810.09462].
- [22] X. Chen, T. Gehrmann, E.W.N. Glover, A. Huss, B. Mistlberger and A. Pelloni, *Fully Differential Higgs Boson Production to Third Order in QCD*, *Phys. Rev. Lett.* **127** (2021) 072002 [2102.07607].
- [23] G. Billis, B. Dehnadi, M.A. Ebert, J.K.L. Michel and F.J. Tackmann, *Higgs p_T Spectrum and Total Cross Section with Fiducial Cuts at Third Resummed and Fixed Order in QCD*, *Phys. Rev. Lett.* **127** (2021) 072001 [2102.08039].
- [24] S. Marzani, R.D. Ball, V. Del Duca, S. Forte and A. Vicini, *Higgs production via gluon-gluon fusion with finite top mass beyond next-to-leading order*, *Nucl. Phys.* **B800** (2008) 127 [0801.2544].
- [25] R.V. Harlander and K.J. Ozeren, *Finite top mass effects for hadronic Higgs production at next-to-next-to-leading order*, *JHEP* **11** (2009) 088 [0909.3420].
- [26] R.V. Harlander, H. Mantler, S. Marzani and K.J. Ozeren, *Higgs production in gluon fusion at next-to-next-to-leading order QCD for finite top mass*, *Eur. Phys. J.* **C66** (2010) 359 [0912.2104].
- [27] A. Pak, M. Rogal and M. Steinhauser, *Finite top quark mass effects in NNLO Higgs boson production at LHC*, *JHEP* **02** (2010) 025 [0911.4662].
- [28] A. Pak, M. Rogal and M. Steinhauser, *Production of scalar and pseudo-scalar Higgs bosons to next-to-next-to-leading order at hadron colliders*, *JHEP* **09** (2011) 088 [1107.3391].
- [29] M. Spira, A. Djouadi, D. Graudenz and P.M. Zerwas, *Higgs boson production at the LHC*, *Nucl. Phys. B* **453** (1995) 17 [hep-ph/9504378].
- [30] R. Harlander and P. Kant, *Higgs production and decay: Analytic results at next-to-leading order QCD*, *JHEP* **12** (2005) 015 [hep-ph/0509189].
- [31] E. Bagnaschi, G. Degrossi, P. Slavich and A. Vicini, *Higgs production via gluon fusion in the POWHEG approach in the SM and in the MSSM*, *JHEP* **02** (2012) 088 [1111.2854].
- [32] R.V. Harlander, T. Neumann, K.J. Ozeren and M. Wiesemann, *Top-mass effects in differential Higgs production through gluon fusion at order α_s^4* , *JHEP* **08** (2012) 139

[1206.0157].

- [33] H. Mantler and M. Wiesemann, *Top- and bottom-mass effects in hadronic Higgs production at small transverse momenta through LO+NLL*, *Eur. Phys. J. C* **73** (2013) 2467 [1210.8263].
- [34] A. Banfi, P.F. Monni and G. Zanderighi, *Quark masses in Higgs production with a jet veto*, *JHEP* **01** (2014) 097 [1308.4634].
- [35] M. Grazzini and H. Sargsyan, *Heavy-quark mass effects in Higgs boson production at the LHC*, *JHEP* **09** (2013) 129 [1306.4581].
- [36] R.V. Harlander, H. Mantler and M. Wiesemann, *Transverse momentum resummation for Higgs production via gluon fusion in the MSSM*, *JHEP* **1411** (2014) 116 [1409.0531].
- [37] T. Neumann and M. Wiesemann, *Finite top-mass effects in gluon-induced Higgs production with a jet-veto at NNLO*, *JHEP* **11** (2014) 150 [1408.6836].
- [38] K. Hamilton, P. Nason and G. Zanderighi, *Finite quark-mass effects in the NNLOPS POWHEG+MiNLO Higgs generator*, *JHEP* **05** (2015) 140 [1501.04637].
- [39] H. Mantler and M. Wiesemann, *Hadronic Higgs production through NLO + PS in the SM, the 2HDM and the MSSM*, *Eur. Phys. J. C* **75** (2015) 257 [1504.06625].
- [40] E. Bagnaschi and A. Vicini, *The Higgs transverse momentum distribution in gluon fusion as a multiscale problem*, *JHEP* **01** (2016) 056 [1505.00735].
- [41] E. Bagnaschi, R.V. Harlander, H. Mantler, A. Vicini and M. Wiesemann, *Resummation ambiguities in the Higgs transverse-momentum spectrum in the Standard Model and beyond*, *JHEP* **01** (2016) 090 [1510.08850].
- [42] R. Frederix, S. Frixione, E. Vryonidou and M. Wiesemann, *Heavy-quark mass effects in Higgs plus jets production*, *JHEP* **08** (2016) 006 [1604.03017].
- [43] T. Neumann and C. Williams, *The Higgs boson at high p_T* , *Phys. Rev. D* **95** (2017) 014004 [1609.00367].
- [44] K. Melnikov and A. Penin, *On the light quark mass effects in Higgs boson production in gluon fusion*, *JHEP* **05** (2016) 172 [1602.09020].
- [45] F. Caola, S. Forte, S. Marzani, C. Muselli and G. Vita, *The Higgs transverse momentum spectrum with finite quark masses beyond leading order*, *JHEP* **08** (2016) 150 [1606.04100].
- [46] J.M. Lindert, K. Melnikov, L. Tancredi and C. Wever, *Top-bottom interference effects in Higgs plus jet production at the LHC*, *Phys. Rev. Lett.* **118** (2017) 252002 [1703.03886].
- [47] T. Liu and A.A. Penin, *High-Energy Limit of QCD beyond the Sudakov Approximation*, *Phys. Rev. Lett.* **119** (2017) 262001 [1709.01092].
- [48] S.P. Jones, M. Kerner and G. Luisoni, *Next-to-Leading-Order QCD Corrections to Higgs Boson Plus Jet Production with Full Top-Quark Mass Dependence*, *Phys. Rev. Lett.* **120** (2018) 162001 [1802.00349].
- [49] F. Caola, J.M. Lindert, K. Melnikov, P.F. Monni, L. Tancredi and C. Wever, *Bottom-quark effects in Higgs production at intermediate transverse momentum*, *JHEP* **09** (2018) 035 [1804.07632].
- [50] X. Chen, A. Huss, S.P. Jones, M. Kerner, J.N. Lang, J.M. Lindert et al., *Top-quark mass effects in $H+jet$ and $H+2 jets$ production*, *JHEP* **03** (2022) 096 [2110.06953].
- [51] M. Czakon, R.V. Harlander, J. Klappert and M. Niggetiedt, *Exact Top-Quark Mass Dependence in Hadronic Higgs Production*, *Phys. Rev. Lett.* **127** (2021) 162002 [2105.04436].

- [52] M. Czakon, F. Eschment, M. Niggetiedt, R. Poncelet and T. Schellenberger, *Top-Bottom Interference Contribution to Fully Inclusive Higgs Production*, *Phys. Rev. Lett.* **132** (2024) 211902 [[2312.09896](#)].
- [53] T. Ježo and P. Nason, *On the Treatment of Resonances in Next-to-Leading Order Calculations Matched to a Parton Shower*, *JHEP* **12** (2015) 065 [[1509.09071](#)].
- [54] F. Cascioli, P. Maierhöfer and S. Pozzorini, *Scattering Amplitudes with Open Loops*, *Phys. Rev. Lett.* **108** (2012) 111601 [[1111.5206](#)].
- [55] F. Buccioni, S. Pozzorini and M. Zoller, *On-the-fly reduction of open loops*, *Eur. Phys. J. C* **78** (2018) 70 [[1710.11452](#)].
- [56] F. Buccioni, J.-N. Lang, J.M. Lindert, P. Maierhöfer, S. Pozzorini, H. Zhang et al., *OpenLoops 2*, *Eur. Phys. J. C* **79** (2019) 866 [[1907.13071](#)].
- [57] T. Ježo, J.M. Lindert, P. Nason, C. Oleari and S. Pozzorini, *An NLO+PS generator for $t\bar{t}$ and Wt production and decay including non-resonant and interference effects*, *Eur. Phys. J. C* **76** (2016) 691 [[1607.04538](#)].
- [58] M.L. Czakon and M. Niggetiedt, *Exact quark-mass dependence of the Higgs-gluon form factor at three loops in QCD*, *JHEP* **05** (2020) 149 [[2001.03008](#)].
- [59] P. Maierhöfer, J. Usovitsch and P. Uwer, *Kira—A Feynman integral reduction program*, *Comput. Phys. Commun.* **230** (2018) 99 [[1705.05610](#)].
- [60] P. Maierhöfer and J. Usovitsch, *Kira 1.2 Release Notes*, [1812.01491](#).
- [61] J. Klappert, F. Lange, P. Maierhöfer and J. Usovitsch, *Integral reduction with Kira 2.0 and finite field methods*, *Comput. Phys. Commun.* **266** (2021) 108024 [[2008.06494](#)].
- [62] J. Klappert and F. Lange, *Reconstructing rational functions with FireFly*, *Comput. Phys. Commun.* **247** (2020) 106951 [[1904.00009](#)].
- [63] J. Klappert, S.Y. Klein and F. Lange, *Interpolation of dense and sparse rational functions and other improvements in FireFly*, *Comput. Phys. Commun.* **264** (2021) 107968 [[2004.01463](#)].
- [64] A.V. Kotikov, *Differential equations method: New technique for massive Feynman diagrams calculation*, *Phys. Lett. B* **254** (1991) 158.
- [65] A.V. Kotikov, *Differential equation method: The Calculation of N point Feynman diagrams*, *Phys. Lett. B* **267** (1991) 123.
- [66] A.V. Kotikov, *Differential equations method: The Calculation of vertex type Feynman diagrams*, *Phys. Lett. B* **259** (1991) 314.
- [67] E. Remiddi, *Differential equations for Feynman graph amplitudes*, *Nuovo Cim. A* **110** (1997) 1435 [[hep-th/9711188](#)].
- [68] S.G. Gorishnii, *Construction of Operator Expansions and Effective Theories in the \overline{MS} Scheme*, *Nucl. Phys. B* **319** (1989) 633.
- [69] V.A. Smirnov, *Asymptotic expansions in limits of large momenta and masses*, *Commun. Math. Phys.* **134** (1990) 109.
- [70] V.A. Smirnov, *Asymptotic expansions in momenta and masses and calculation of Feynman diagrams*, *Mod. Phys. Lett. A* **10** (1995) 1485 [[hep-th/9412063](#)].
- [71] V.A. Smirnov, *Applied asymptotic expansions in momenta and masses*, *Springer Tracts Mod. Phys.* **177** (2002) 1.
- [72] R. Bonciani, V. Del Duca, H. Frellesvig, J.M. Henn, F. Moriello and V.A. Smirnov, *Two-loop*

- planar master integrals for $Higgs \rightarrow 3$ partons with full heavy-quark mass dependence, *JHEP* **12** (2016) 096 [[1609.06685](#)].
- [73] R. Bonciani, V. Del Duca, H. Frellesvig, J.M. Henn, M. Hidding, L. Maestri et al., *Evaluating a family of two-loop non-planar master integrals for Higgs + jet production with full heavy-quark mass dependence*, *JHEP* **01** (2020) 132 [[1907.13156](#)].
- [74] H. Frellesvig, M. Hidding, L. Maestri, F. Moriello and G. Salvatori, *The complete set of two-loop master integrals for Higgs + jet production in QCD*, *JHEP* **06** (2020) 093 [[1911.06308](#)].
- [75] M. Niggetiedt and J. Usovitsch, *The Higgs-gluon form factor at three loops in QCD with three mass scales*, *JHEP* **02** (2024) 087 [[2312.05297](#)].
- [76] T. Becher and M. Neubert, *Infrared singularities of scattering amplitudes in perturbative QCD*, *Phys. Rev. Lett.* **102** (2009) 162001 [[0901.0722](#)].
- [77] T. Becher and M. Neubert, *On the Structure of Infrared Singularities of Gauge-Theory Amplitudes*, *JHEP* **06** (2009) 081 [[0903.1126](#)].
- [78] D. Lombardi, M. Wiesemann and G. Zanderighi, *Advancing $MiNNLO_{PS}$ to diboson processes: $Z\gamma$ production at $NNLO+PS$* , *JHEP* **06** (2021) 095 [[2010.10478](#)].
- [79] D. Lombardi, M. Wiesemann and G. Zanderighi, *W^+W^- production at $NNLO+PS$ with $MiNNLO_{PS}$* , *JHEP* **11** (2021) 230 [[2103.12077](#)].
- [80] L. Buonocore, G. Koole, D. Lombardi, L. Rottoli, M. Wiesemann and G. Zanderighi, *ZZ production at $nNNLO+PS$ with $MiNNLO_{PS}$* , *JHEP* **01** (2022) 072 [[2108.05337](#)].
- [81] D. Lombardi, M. Wiesemann and G. Zanderighi, *Anomalous couplings in $Z\gamma$ events at $NNLO+PS$ and improving $\nu\bar{\nu}\gamma$ backgrounds in dark-matter searches*, *Phys. Lett. B* **824** (2022) 136846 [[2108.11315](#)].
- [82] S. Zanolini, M. Chiesa, E. Re, M. Wiesemann and G. Zanderighi, *Next-to-next-to-leading order event generation for VH production with $H \rightarrow b\bar{b}$ decay*, *JHEP* **07** (2022) 008 [[2112.04168](#)].
- [83] A. Gavardi, C. Oleari and E. Re, *$NNLO+PS$ Monte Carlo simulation of photon pair production with $MiNNLO_{PS}$* , [2204.12602](#).
- [84] U. Haisch, D.J. Scott, M. Wiesemann, G. Zanderighi and S. Zanolini, *$NNLO$ event generation for $pp \rightarrow Zh \rightarrow \ell^+\ell^-\bar{b}b$ production in the SM effective field theory*, *JHEP* **07** (2022) 054 [[2204.00663](#)].
- [85] J.M. Lindert, D. Lombardi, M. Wiesemann, G. Zanderighi and S. Zanolini, *WZ production at $NNLO$ QCD and NLO EW matched to parton showers with $MiNNLO_{PS}$* , *JHEP* **11** (2022) 036 [[2208.12660](#)].
- [86] C. Biello, A. Sankar, M. Wiesemann and G. Zanderighi, *$NNLO+PS$ predictions for Higgs production through bottom-quark annihilation with $MiNNLO_{PS}$* , *Eur. Phys. J. C* **84** (2024) 479 [[2402.04025](#)].
- [87] J. Mazzitelli, P.F. Monni, P. Nason, E. Re, M. Wiesemann and G. Zanderighi, *Next-to-Next-to-Leading Order Event Generation for Top-Quark Pair Production*, *Phys. Rev. Lett.* **127** (2021) 062001 [[2012.14267](#)].
- [88] J. Mazzitelli, P.F. Monni, P. Nason, E. Re, M. Wiesemann and G. Zanderighi, *Top-pair production at the LHC with $MiNNLO_{PS}$* , *JHEP* **04** (2022) 079 [[2112.12135](#)].
- [89] J. Mazzitelli, A. Ratti, M. Wiesemann and G. Zanderighi, *B -hadron production at the LHC from bottom-quark pair production at $NNLO+PS$* , *Phys. Lett. B* **843** (2023) 137991

[2302.01645].

- [90] J. Mazzeiti, V. Sotnikov and M. Wiesemann, *Next-to-next-to-leading order event generation for Z-boson production in association with a bottom-quark pair*, [2404.08598](#).
- [91] P. Nason, *A New method for combining NLO QCD with shower Monte Carlo algorithms*, *JHEP* **11** (2004) 040 [[hep-ph/0409146](#)].
- [92] P. Nason and G. Ridolfi, *A Positive-weight next-to-leading-order Monte Carlo for Z pair hadroproduction*, *JHEP* **08** (2006) 077 [[hep-ph/0606275](#)].
- [93] S. Frixione, P. Nason and C. Oleari, *Matching NLO QCD computations with Parton Shower simulations: the POWHEG method*, *JHEP* **11** (2007) 070 [[0709.2092](#)].
- [94] S. Alioli, P. Nason, C. Oleari and E. Re, *A general framework for implementing NLO calculations in shower Monte Carlo programs: the POWHEG BOX*, *JHEP* **06** (2010) 043 [[1002.2581](#)].
- [95] NNPDF collaboration, *Parton distributions from high-precision collider data*, *Eur. Phys. J.* **C77** (2017) 663 [[1706.00428](#)].
- [96] T. Sjöstrand, S. Ask, J.R. Christiansen, R. Corke, N. Desai, P. Ilten et al., *An Introduction to PYTHIA 8.2*, *Comput. Phys. Commun.* **191** (2015) 159 [[1410.3012](#)].
- [97] ATLAS collaboration, *Measurement of the total and differential Higgs boson production cross-sections at $\sqrt{s} = 13$ TeV with the ATLAS detector by combining the $H \rightarrow ZZ^* \rightarrow 4\ell$ and $H \rightarrow \gamma\gamma$ decay channels*, *JHEP* **05** (2023) 028 [[2207.08615](#)].
- [98] G.P. Salam and E. Slade, *Cuts for two-body decays at colliders*, *JHEP* **11** (2021) 220 [[2106.08329](#)].
- [99] M. Grazzini, S. Kallweit and M. Wiesemann, *Fully differential NNLO computations with MATRIX*, *Eur. Phys. J.* **C78** (2018) 537 [[1711.06631](#)].